GEOPHYSICS, VOL. 58, NO. 4 (APRIL 1993); P. 524–533, 6 FIGS.

Dynamic poroelasticity: A unified model with the squirt and the Biot mechanisms

Jack Dvorkin* and Amos Nur*

ABSTRACT

The velocities and attenuation of seismic and acoustic waves in rocks with fluids are affected by the two most important modes of fluid/solid interaction: (1) the Biot mechanism where the fluid is forced to participate in the solid's motion by viscous friction and inertial coupling, and (2) the squirt-flow mechanism where the fluid is squeezed out of thin pores deformed by a passing wave. Traditionally, both modes have been modeled separately, with the Biot mechanism treated in a macroscopic framework, and the squirt flow examined at the individual pore level. We offer a model which treats both mechanisms as coupled processes and relates *P*-velocity and attenuation to macroscopic parameters: the Biot poroelastic constants, porosity, permeability, fluid compressibility and viscosity, and a newly introduced microscale parameter—a characteristic squirt-flow length. The latter is referred to as a fundamental rock property that can be determined experimentally. We show that the squirt-flow mechanism dominates the Biot mechanism and is responsible for measured large velocity dispersion and attenuation values. The model directly relates *P*-velocity and attenuation to measurable rock and fluid properties. Therefore, it allows one to realistically interpret velocity dispersion and/or attenuation in terms of fluid properties changes [e.g., viscosity during thermal enhanced oil recovery (EOR)], or to link seismic measurements to reservoir properties. As an example of the latter transformation, we relate permeability to attenuation and achieve good qualitative correlation with experimental data.

INTRODUCTION

The theories of quasi-static and dynamic poroelasticity presented by Biot (1941 and 1956) have served as rigorous and formal foundations to numerous practical solutions concerning the stability of constructions on consolidating soils (e.g., Biot, 1942), stress diffusion around pressurized cavities (Rice and Cleary, 1976), and acoustic wave propagation in saturated sediments (e.g., Stoll, 1974).

Burridge and Keller (1981) generalize the Biot theory for a porous elastic solid with a compressible viscous fluid. Their derivations are based on the equations of linear elasticity in the solid, and the linearized Navier-Stokes equations in the fluid. When the viscosity of the fluid is small, the resulting general equations become those of Biot.

In Biot's model, pore fluid is forced to participate in a solid's oscillatory motion by viscous friction and inertial coupling. A different mechanism of fluid flow during seismic and acoustic wave propagation is associated with the squirting of the pore fluid out of cracks as they are deformed by passing seismic waves. Mavko and Nur (1979) have shown that the squirt-flow mechanism results in much higher and realistic attenuation values in partially saturated rocks than those predicted by Biot's mechanism. Mavko and Nur (1975) have suggested that squirt may occur even in fully saturated rocks due to fluid flowing between saturated cracks of different orientation. This mechanism has been shown to be responsible for the measured seismic energy losses and velocity dispersion in sedimentary materials for both *P*- and *S*-waves (e.g., Murphy et al., 1986; Wang and Nur, 1990).

The squirt-flow mechanism has been traditionally investigated by examining fluid flow in an individual crack (e.g., Mavko and Nur, 1979; Miksis, 1988) or at a grain contact point (Palmer and Traviolia, 1980). Attenuation and velocities have been calculated by considering viscous energy losses or through a complex modulus (e.g., Murphy et al., 1986). By so doing, workers have treated the squirt-flow mechanism independent of Biot's mechanism. Yet, it is clear that these two modes of solid/fluid interaction are intimately interconnected via fluid mass balance. Occurring

Manuscript received by the Editor March 13, 1992; revised manuscript received October 7, 1992.
*Department of Geophysics, Stanford University, Stanford, CA 94305-2215.

in a rock simultaneously, they will effect each other, as well as influence the process of seismic energy propagation and attenuation. Therefore, a consistent theory dealing simultaneously with the Biot and the squirt-flow mechanisms has to take into account the possibility of the fluid's motion both parallel (the Biot mechanism) and transverse (the squirt-flow mechanism) to the direction of a planar P-wave propagation (Figure 1a).

We offer a heuristic model for the Biot/squirt (BISQ) flow in rocks. Once a scheme of these two mechanisms occurring simultaneously is accepted, the mathematical formalization of the process follows, which yields governing wave equations. Here, we consider P-waves only, as shear velocity and attenuation will be examined later.

We assume that the rock deforms in the uniaxial mode (Figure 1a), i.e., the only nonzero component of the deformation of the solid skeleton is in the direction of wave propagation. The fluid, however, is free to move not only parallel but also perpendicular to this direction. This fluid flow is induced by the compression of pore volume due to wave excitation, which results in increasing pore pressure. For pressure gradient to develop, we assume that pore pressure on the sides of a small homogeneous representative volume of the rock does not change in time. The most natural choice of the representative volume for the case under consideration is a cylinder with its axis parallel to the direction of wave propagation (Figures 1a and 1b). The radius of this cylinder is a characteristic squirt-flow length that has the order of the average pore size. We assume that this microscale parameter is a fundamental rock property and thus does not depend on frequency and fluid properties.

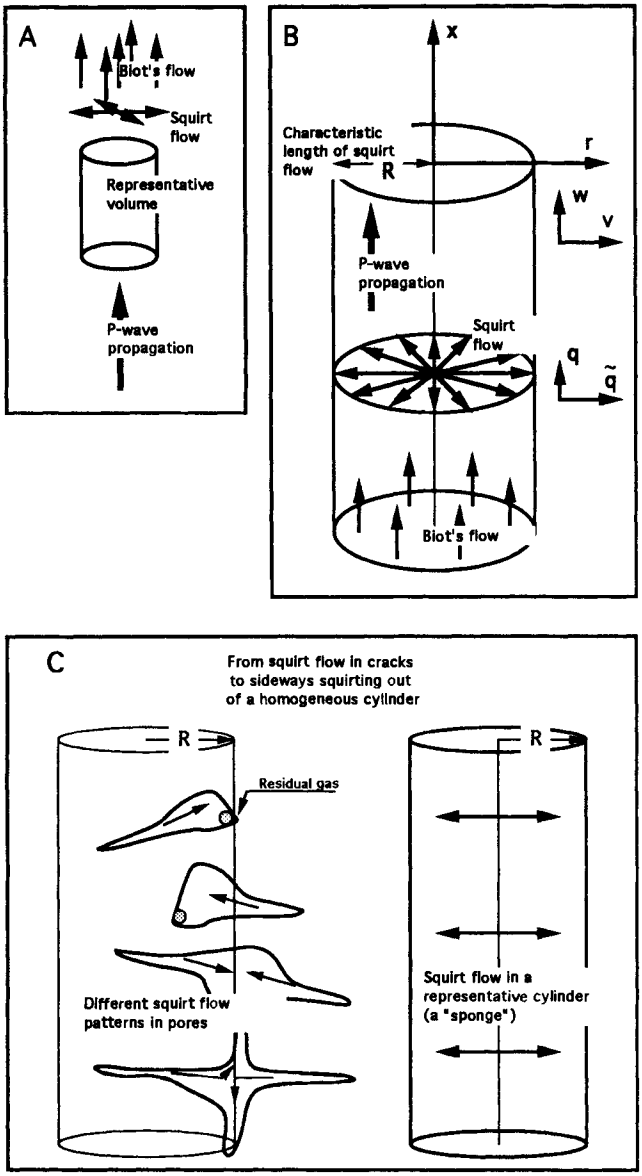

FIG. 1. The BISQ model. (a) Biot's flow and squirt flow in a rock due to seismic excitation. (b) A cylindrical representative volume of a rock. (c) From squirt flow in cracks to the "sponge" model.

In this model, the attenuation is due to viscous friction losses in the fluid. Indeed, this mechanism appears to dominate seismic wave scattering even at frequencies as high as 1 MHz (Wepfer and Cristensen, 1990). We show that the BISQ model yields much higher and realistic attenuation, as well as velocity dispersion values, than the Biot theory.

The effect of fluid flow transverse to the direction of wave propagation is investigated by Gardner (1962) in his theory of extensional waves in fluid-saturated porous cylinders. The solution presented here is different, as we explicitly examine the propagation of P-waves in an infinite medium and thus deal with the effective dynamic plane-wave modulus of rocks with fluids. The novelty of our concept is in expressing the effect of local (squirt) flow through fundamental measurable rock and fluid properties. Our derivation of the wave equations and their solution results in simple practical formulas for V_P and attenuation.

The BISQ model relates the dynamic poroelastic behavior of a saturated rock to traditional poroelastic constants, porosity, permeability, fluid compressibility and viscosity, and the characteristic squirt flow length. These parameters are combined in two expressions, one of which is the Biot's characteristic frequency and the other includes the characteristic squirt flow length. Therefore, the model allows us to relate P-velocity and attenuation to rock and fluid properties, the most important of which are permeability, porosity, viscosity, and compressibility. As an example, we relate permeability to attenuation and achieve good qualitative correlation with experimental data.

DYNAMIC POROELASTICITY (BIOT'S THEORY)

In this section, we introduce the dynamic poroelasticity relations following Biot (1941 and 1956) and Rice and Cleary (1976). We examine the uniaxial deformation of a porous rock assuming that both solid and fluid move only in the direction of P-wave propagation. We also assume that the rock is homogeneous and isotropic.

Stresses and dynamic equations

For uniaxial deformation in the x-direction (Figure 1b), stresses in the skeleton σ_x, the skeleton's displacement u and fluid pressure P are related as (Appendix):

$$\sigma_x = M\frac{du}{dx} - \gamma P, \tag{1}$$

where $\gamma = \alpha - \phi$, ϕ is the porosity of the rock, α is the poroelastic coefficient,

$$M = 2G\frac{1-\nu}{1-2\nu},\quad \alpha = \frac{2(1+\nu)}{3(1-2\nu)}\frac{G}{H} = 1 - \frac{K}{K_s},$$

$$\frac{1}{H} = \frac{1}{K} - \frac{1}{K_s}.$$

M, K, and G are the uniaxial, the bulk, and the shear moduli of the skeleton in drained conditions, ν is its Poisson's ratio, and K_s is the bulk modulus of the solid phase.

The Biot (1956) dynamic equations for a two-component solid-fluid continuum and formula (1) yield (Appendix):

$$(1-\phi)\rho_s u_{tt} + \phi\rho_f w_{tt} = Mu_{xx} - \alpha P_x,$$

$$\phi\rho_f w_{tt} - \rho_a(u_{tt} - w_{tt}) - \frac{\mu\phi^2}{k}(u_t - w_t) = -\phi P_x, \qquad (2)$$

where t is time, w is the fluid's displacement in the x-direction, ρ_s is the density of the solid (grain) material, ρ_f is the density of the fluid, ρ_a is the additional coupling density, μ is the viscosity of the fluid, k is the permeability of the skeleton, subscripts x and t indicate partial derivatives ($P_x = \partial P/\partial x$, $u_{tt} = \partial^2 u/\partial t^2$, etc.).

Pressure in the fluid

The equation of the fluid's mass conservation in the porous rock moving with velocity u_t

$$\frac{\partial(\rho_f\phi)}{\partial t} + \frac{\partial[\rho_f(q - \phi u_t)]}{\partial x} = 0,$$

with the fluid's volumetric filtration rate in the x-direction, q related to the fluid's displacement w as $q = \phi w_t$, gives, after linearization:

$$\frac{\phi}{\rho_f}\frac{\partial\rho_f}{\partial t} + \frac{\partial\phi}{\partial t} + \phi\frac{\partial^2(w-u)}{\partial x\partial t} = 0. \qquad (3)$$

Porosity differential is related to the differentials of the skeleton's deformation ($e = du/dx$) and of the fluid's pressure as (Biot, 1941; Rice and Cleary, 1976):

$$d\phi = \alpha de + dP/Q,$$

$$\frac{1}{Q} = \frac{1-\alpha}{K} - \frac{1-\alpha+\phi}{K_s} = \frac{1}{K_s}\left(1 - \phi - \frac{K}{K_s}\right).$$

Therefore,

$$\frac{\partial\phi}{\partial t} = \alpha\frac{\partial^2 u}{\partial x\partial t} + \frac{1}{Q}\frac{\partial P}{\partial t}. \qquad (4)$$

We describe the fluid's compressibility by a linear relation

$$d\rho_f = dP/c_0^2, \qquad (5)$$

where c_0 is fluid acoustic velocity.

By substituting equations (4) and (5) into equation (3), we relate pressure P to displacements u and w as:

$$P_t = -F\left(w_{xt} + \frac{\gamma}{\phi}u_{xt}\right), \qquad (6)$$

where

$$F = \left(\frac{1}{\rho_f c_0^2} + \frac{1}{\phi Q}\right)^{-1}.$$

P-velocity and attenuation

The system of three differential equations (2) and (6) contains three variables u, w, and P. We solve it to find the velocity V_P and attenuation coefficient a of a planar P-wave. The solution yields two values for P-velocity (the fast wave and the slow wave) and two corresponding values for attenuation (Appendix):

$$V_{P1,2} = \frac{1}{\mathrm{Re}\,(X_{1,2})},\quad a_{1,2} = \omega\,\mathrm{Im}\,(X_{1,2}), \qquad (7)$$

where ω is the angular frequency, $\omega_c = \mu\phi/k\rho_f$,

$$X_{1,2} = \sqrt{Y_{1,2}},\quad Y_{1,2} = -\frac{B}{2A} \pm \sqrt{\left(\frac{B}{2A}\right)^2 - \frac{C}{A}},$$

$$A = \frac{\phi FM}{\rho_2^2},\quad B = \frac{F\left(2\alpha - \phi - \phi\frac{\rho_1}{\rho_2}\right) - \left(M + F\frac{\alpha^2}{\phi}\right)\left(1 + \frac{\rho_a}{\rho_2} + i\frac{\omega_c}{\omega}\right)}{\rho_2},$$

$$C = \frac{\rho_1}{\rho_2} + \left(1 + \frac{\rho_1}{\rho_2}\right)\left(\frac{\rho_a}{\rho_2} + i\frac{\omega_c}{\omega}\right),$$

where

$$\rho_1 = (1-\phi)\rho_s,\ \rho_2 = \phi\rho_f,\ \omega_c = \mu\phi/k\rho_f.$$

INTRODUCING SQUIRT FLOW (THE BISQ THEORY)

The model

To incorporate the squirt-flow mechanism in the dynamic poroelasticity model, we assume that the solid skeleton of a rock deforms in the uniaxial mode parallel to the direction of wave propagation. The fluid, however, can flow not only parallel (Biot's flow), but also perpendicular (squirt flow) to this direction (Figure 1a). We model this sideways flow in the r-direction by examining a representative cylindrical volume of the rock with the axis in the direction of wave propagation. Pressure on the external surface of this cylinder at $r = R$ (Figure 1b) does not change in time, so that the fluid can be squeezed out or pumped in when the rock is compressed or extended due to wave excitation. The radius of this

cylinder is the average squirt flow length—a microscale parameter that is assumed to be a fundamental property of a rock and thus does not depend on frequency, and fluid viscosity and compressibility.

A simple way of viewing this model is to imagine a cylindrical sponge filled with fluid and uniaxially compressed along the x-direction (Figure 1b). Fluid pressure at the lateral surface of the sponge is assumed to be constant and equal to the initial pore pressure. As the sponge undergoes compression, the fluid will flow in directions both parallel and perpendicular to the x-axis. The latter (squirt) flow component may result in large fluid pressure fluctuations, which in turn will affect the poroelastic response of the sponge to external loading. This model accommodates squirting flow patterns proposed by different authors (e.g., Mavko and Nur, 1975; Johnston et al., 1979). It allows us to characterize squirt flow by only two parameters: permeability in the radial direction and the radius of the representative cylinder instead of considering cracks of various shapes and sizes (Figure 1c).

The condition of constant pressure on the external surface of a representative cylinder is strictly valid in apparently fully saturated rocks with only small amounts of high compressibility gas in the pores. This situation is often the case in natural reservoirs. The squirt-flow pattern becomes more complicated in saturated rocks without residual gas: pore fluid is pushed from thin cracks into the surrounding large pores with pressure in these pores changing in time. In this case, the BISQ model will also give realistic quantitative estimates to attenuation and velocity dispersion, as pressure variation in large pores is much smaller than that in thin cracks.

The mathematical implementation of our BISQ model is based on the equations of solid/fluid dynamic interaction (Biot, 1956) which include the displacements of the solid and the fluid, as well as fluid pressure. To link the latter variable to the squirt flow mechanism, we examine a two-dimensional (2-D) axisymmetrical flow of the fluid induced by the solid's deformation. The pressure of the fluid $P(t, x, r)$ is found from the equation of the fluid's mass balance. It depends on time t, as well as on both the x and the r coordinates (Figure 1b). To use this 2-D pressure distribution in the one-dimensional (1-D) equations of solid/fluid interaction, we calculate its average value with respect to the r-direction. This average value depends only on t and x and can be immediately substituted into the solid/fluid interaction equations. By analyzing these equations, we find both the fast and the slow compressional velocities, as well as corresponding attenuations.

Squirt flow: Two-dimensional axisymmetrical filtration

In the case under consideration, we have to examine the 2-D axisymmetrical equation of the fluid's mass conservation with the volumetric filtration rate $\bar{q}$ in the r-direction taken into account:

$$\frac{\partial(\rho_f\phi)}{\partial t} + \frac{\partial[\rho_f(q - \phi u_t)]}{\partial x} + \frac{\partial(\rho_f\bar{q})}{\partial r} + \frac{\rho_f\bar{q}}{r} = 0, \qquad (8)$$

where $\bar{q}$ is related to the fluid's displacement v in the r-direction as $\bar{q} = \phi v_t$. Retaining only linear terms in equation (8) yields:

$$\frac{\phi}{\rho_f}\frac{\partial\rho_f}{\partial t} + \frac{\partial\phi}{\partial t} + \phi\frac{\partial^2(w-u)}{\partial x\partial t} + \phi\left(\frac{\partial^2 v}{\partial r\partial t} + \frac{1}{r}\frac{\partial v}{\partial t}\right) = 0. \qquad (9)$$

This equation generalizes equation (3) for the case of 2-D axisymmetrical fluid flow.

By substituting equations (4) and (5) into equation (9) we relate pressure P to displacements u, v, and w:

$$P_t = -F\left(w_{xt} + v_{rt} + \frac{1}{r}v_t + \frac{\gamma}{\phi}u_{xt}\right). \qquad (10)$$

This equation is analogous to equation (6) which was derived for the case of 1-D fluid flow.

Dynamic equations

In the case under consideration, we have one dynamic equation in the r-direction in addition to equations (2) in the x-direction. This equation can be derived from Lagrange's equations with a dissipation function (Biot, 1956):

$$(\phi\rho_f + \rho_a)v_{tt} + \frac{\mu\phi^2}{k}v_t = -\phi P_r. \qquad (11)$$

We are looking for the solution of our problem in the following form:

$$v(x, r, t) = v_0(r)e^{i(\ell x - \omega t)},$$
$$P(x, r, t) = P_0(r)e^{i(\ell x - \omega t)}. \qquad (12)$$

Substituting equation (12) into equation (11), we relate radial fluid displacement to pressure gradient as

$$\frac{\partial P_0}{\partial r} = v_0\rho_f\omega^2\left(\frac{\phi + \rho_a/\rho_f}{\phi} + i\frac{\omega_c}{\omega}\right). \qquad (13)$$

Pressure in the fluid

We assume here that both the displacement of the solid and the displacement of the fluid in the x-direction are affected by values of P and v averaged with respect to r. In other words, only average local flow parameters affect the global Biot's flow. Therefore, we can again present the solid's displacement u and the fluid's displacement w in the x-direction as:

$$u(x, t) = C_1 e^{i(\ell x - \omega t)},$$
$$w(x, t) = C_2 e^{i(\ell x - \omega t)}, \qquad (14)$$

where C_1 and C_2 are constants (Appendix).

Using equations (12)–(14), we transform equation (10) into an ordinary differential equation which describes fluid pressure dependence on the r coordinate:

$$\frac{d^2P_0}{dr^2} + \frac{1}{r}\frac{dP_0}{dr} + P_0\frac{\rho_f\omega^2}{F}\left(\frac{\phi + \rho_a/\rho_f}{\phi} + i\frac{\omega_c}{\omega}\right) = -i\ell(\gamma C_1 + \phi C_2)\frac{\rho_f\omega^2}{\phi}\left(\frac{\phi + \rho_a/\rho_f}{\phi} + i\frac{\omega_c}{\omega}\right).$$

We solve this equation with a constant pressure boundary condition (for example, $P_0 = 0$) at $r = R$, where R is the

radius of the representative cylindrical volume and is equal to the characteristic squirt flow length (Figure 1b). The solution is:

$$P_0 = -i\ell(\gamma C_1 + \phi C_2)\frac{F}{\phi}\left[1 - \frac{J_0(\lambda r)}{J_0(\lambda R)}\right],$$

where J_0 is the Bessel function of zero order and

$$\lambda^2 = \frac{\rho_f \omega^2}{F}\left(\frac{\phi + \rho_a/\rho_f}{\phi} + i\frac{\omega_c}{\omega}\right).$$

Average fluid pressure can be found from the previous equation and relations (12) and (14):

$$P_{av} = \frac{1}{\pi R^2}\int_0^R 2\pi r P(x, r, t)\, dr$$

$$= -F\left[1 - \frac{2J_1(\lambda R)}{\lambda R J_0(\lambda R)}\right]\left(w_x + \frac{\gamma}{\phi}u_x\right), \quad (15)$$

where J_1 is the Bessel function of first order. Taking derivatives with respect to t we find from equation (15):

$$\frac{\partial P_{av}}{\partial t} = -F\left[1 - \frac{2J_1(\lambda R)}{\lambda R J_0(\lambda R)}\right]\left(w_{xt} + \frac{\gamma}{\phi}u_{xt}\right). \quad (16)$$

P-velocity and attenuation

As we mentioned before, it is assumed that the average local flow pressure P_{av} can be used as the actual fluid pressure P in dynamic equations (2). Therefore, if the effect of squirt flow is taken into account, equation (16) rather than equation (6) has to be used with equations (2). The only difference between equations (6) and (16) is in the proportionality coefficient that relates the derivative of pressure to the derivatives of the fluid's and the solid's displacements. Namely, coefficient

$$F_{sq} = F\left[1 - \frac{2J_1(\lambda R)}{\lambda R J_0(\lambda R)}\right] \quad (17)$$

has to be used instead of F.

This means that equation (7) can be used for calculating velocities and attenuations when both the Biot and the squirt mechanisms are taken into consideration. The values of $X_{1,2}$, $Y_{1,2}$, A, B, and C have to be calculated by using F_{sq} instead of F.

THE BISQ MODEL: ANALYSIS AND DISCUSSION

The principal difference between our BISQ model and the Biot model is in considering the variation in fluid dynamic pressure due to squirt flow. As we will show below, this consideration significantly changes such characteristics of the poroelastic response of a saturated rock to acoustic wave propagation as velocity dispersion and attenuation. Yet, in mathematical formulation, the BISQ model naturally continues the original Biot theory. The only formal difference is in the coefficient that relates fluid pressure to the solid's and the fluid's displacement in the direction of wave propagation. This coefficient F is constant in the original Biot case, whereas it becomes frequency dependent (F_{sq}) in the BISQ model. In the first case, a single constant ω_c (the angular characteristic Biot's frequency) determines the dependence of velocities and attenuations on frequency: these parameters depend on ratio

$$\frac{\omega_c}{\omega} = \frac{\mu\phi}{k\rho_f\omega}. \quad (18)$$

In the second case, we introduce an additional new parameter

$$\lambda R = \sqrt{R^2\frac{\rho_f\omega^2}{F}\left(\frac{\phi + \rho_a/\rho_f}{\phi} + i\frac{\omega_c}{\omega}\right)} \quad (19)$$

which includes the characteristic squirt-flow length R.

It is clear from (17) that F_{sq} approaches F and thus the results of the BISQ theory converge with the results of the Biot theory as R increases. Indeed, as the characteristic squirt flow length grows, local inhomogeneities in the r-direction that cause the squirt-flow phenomenon (Figure 1c) disappear, and the flow becomes essentially 1-D, as suggested by the Biot model.

Approximate expressions for V_P and Q^{-1}

Consider the case

$$\frac{\omega_c}{\omega} = \frac{\mu\phi}{k\rho_f\omega} \gg 1, \quad (20)$$

which may be of practical importance even for high frequencies. Indeed, for a water-saturated rock of $\phi = 0.2$ and $k = 10$ md, and using $\mu = 1$ mPa · s and $\rho_f = 1000$ kg/m^3, we find $\omega_c/\omega = 2 \cdot 10^7/\omega$, and the above condition is satisfied even for 0.1 MHz frequency.

By using equation (20), we can find the following approximate expressions for V_P and a from equations (7) and (17):

$$V_P = \frac{1}{\text{Re}\,(\sqrt{Y})},\quad a = \omega\ \text{Im}\,(\sqrt{Y}), \quad (21)$$

where

$$Y = \frac{\rho_s(1-\phi) + \rho_f\phi}{M + F_{sq}\alpha^2/\phi},\quad F_{sq} = F\left[1 - \frac{2J_1(\xi)}{\xi J_0(\xi)}\right],$$

$$\xi = \sqrt{i}\sqrt{\frac{R^2\omega}{\kappa}},\quad \kappa = \frac{kF}{\mu\phi}. \quad (22)$$

The inverse quality factor Q^{-1} is related to a and V_P as:

$$Q^{-1} = 2aV_P/\omega.$$

In this case, instead of equations (18) and (19), we have only one group that determines the poroelastic response of a rock:

$$\xi = \sqrt{i}\sqrt{\frac{R^2\omega}{\kappa}},\quad \kappa = \frac{kF}{\mu\phi}. \quad (23)$$

Low- and high-frequency limits

Following the Biot theory we find from equation (7) that for low frequencies ($\omega \to 0$) P-velocity is:

$$V_{P0} = \sqrt{\frac{M + \alpha^2 F/\phi}{(1-\phi)\rho_s + \phi\rho_f}},$$

which is in fact the Gassmann formula (White, 1983).

The BISQ model yields $F_{sq} \to 0$ as $\omega \to 0$. Therefore,

$$V_{p0} = \sqrt{\frac{M}{(1-\phi)\rho_s + \phi\rho_f}}.$$

Thus the P-velocity low-frequency limit obtained from the BISQ model is lower than that obtained from the Biot theory. It is equal to the P-velocity in a material with the uniaxial modulus of the skeleton M and the density $\rho = (1 - \phi)\rho_s + \phi\rho_f$ which is the composite density of a saturated porous medium. This result follows from the boundary condition on the surface of the representative cylinder ($P = 0$). It can be easily interpreted if we consider the fact that at low frequencies the fluid is slowly and easily squeezed perpendicular to the direction of wave propagation and thus does not contribute to the response of the saturated medium to acoustic excitation.

As $\omega \to \infty$, λ in equation (17) also approaches infinity and

$$F_{sq} = F\left[1 - \frac{2J_1(\lambda R)}{\lambda R J_0(\lambda R)}\right] \to F,$$

which means that the high-frequency limits are identical in both the Biot and the BISQ theories. This result is also physically clear, because at high frequencies the fluid behaves in the unrelaxed mode and cannot be squeezed out of the pore space to produce the squirt flow effect.

In deriving this high-frequency limit, we ignore viscous coupling of fluids near the pore walls that causes viscosity μ to be frequency dependent (Biot, 1956). This approximate treatment is justified for the BISQ model as the transition between low-frequency and high-frequency velocity values occurs at frequencies that are well below the Biot characteristic frequency (see examples below). Using the same reasoning, we also neglect scattering losses from individual pores and grains (Wepfer and Cristensen, 1990).

The above results indicate that velocity dispersion as predicted by the BISQ theory is larger than that resulting from the Biot theory. The following numerical example shows that this difference can be significant and can result in much higher and realistic attenuation values than those predicted by the Biot theory.

The BISQ low-frequency limit does not contradict the Gassmann formula because the former is strictly valid only for apparently fully saturated rocks. The important result of the BISQ model is the large velocity dispersion. This dispersion estimate will hold even for rocks without residual gas (see previous above).

Characteristic squirt flow length

The physical meaning of the characteristic squirt-flow length R is the average length that gives a squirt-flow effect identical to the cumulative effect of local flow in pores of various shapes and sizes. R is intimately related to the pore space geometry of a given rock. We assume that this parameter is a fundamental property of a rock and can be determined experimentally.

To clarify this statement, we use as an analogy the Darcy law that states that permeability is a fundamental rock property and does not depend on the type of fluid and pressure gradient. Permeability cannot be measured directly, but can be calculated by matching the Darcy formula with experimental measurements of fluid flow rate versus pressure gradient. Once permeability value is determined, it can be used for a given rock to calculate the flow rates of various fluids versus various pressure gradients.

A similar rule applies to determining the characteristic squirt-flow length: R can be calculated by matching formulas (7) and (17) or, for simplicity, formula (21) to experimental measurements of V_P and/or Q^{-1} in a rock of known porosity, permeability, and dry skeleton properties saturated with a fluid of known density, viscosity, and compressibility. Below, we offer a numerical example where R is found from matching theoretical to experimental results.

The geometry in the BISQ model

In the BISQ model, we avoid the dependence of the squirt-flow effect on the individual pore geometry by averaging this effect among pores of various shapes and sizes. We achieve this result by using two fundamental parameters: permeability and the characteristic squirt-flow length. The final formulas for V_P and Q^{-1} depend only on the geometry of the representative volume of a rock that we assume to be a cylinder. This choice is dictated by the nature of the problem under consideration: the propagation of a planar compressional wave. This representative volume will be a sphere when we consider bulk compression.

NUMERICAL EXAMPLES

We examine the effects of frequency and characteristic squirt length on velocity and attenuation in a water-saturated 15 percent porosity rock. The elastic characteristics of the skeleton are: K = 16 GPa and Poisson's ratio 0.15. The density of the solid phase is 2650 kg/m^3, its bulk modulus K_s = 38 GPa. The additional coupling density is chosen 420 kg/m^3, according to Berryman's (1980) formula.

The effect of frequency

To investigate the effect of frequency on seismic velocities and attenuation, we examine three cases with permeability equal to 1.25, 2.5, and 5 md. Characteristic frequencies for these cases are 19.1 MHz, 9.55 MHz, and 4.77 MHz, respectively. The characteristic squirt length is chosen 1 mm. The velocity-frequency curves for these three cases are given in Figure 2a. V_P changes from its low-frequency limit to the high-frequency limit as frequency increases. The transition zone shifts towards high frequencies as permeability increases. This trend can also be observed on Q^{-1} versus frequency curves (Figure 3a) where the attenuation peak shifts towards high frequencies with increasing permeability. This result is physically clear because the squirting motion of the fluid becomes unrelaxed at lower frequencies for lower

permeabilities. It is important to notice that in all three cases the maximum attenuation due to the combined Biot/squirt effect is at frequencies that are well below the characteristic frequency values f_c ($\text{Log}\, f_c$ = 7.28, 6.98, and 6.68, correspondingly).

Comparing these results to the results of using the original Biot theory (Figures 2b and 3b), we find that both velocity dispersion and attenuation are significantly smaller than predicted by the BISQ model. This effect gives one explanation for the experimental results observed by Wang and Nur (1990) where the apparent V_P dispersion versus permeability was an order of magnitude higher than that predicted by Biot's theory.

Another important result is that attenuation peaks and velocity transition zones shift towards high frequencies as permeability increases. This effect is opposite to the trend predicted by the Biot theory. It can be explained by the fact that in the original Biot theory V_P and Q^{-1} depend on the ratio $\omega_c/\omega = \mu\phi/k\omega\rho_f$ and thus on the product ωk. In the BISQ model, V_P and Q^{-1} depend on the combination $R^2\omega\mu\phi/kF$, as follows from simplified formula (23), and thus on the ratio ω/k.

The effect of characteristic squirt length

The effect of characteristic squirt length R on V_P and Q^{-1} is examined at frequency 10 kHz for permeabilities 1.25, 2.5, and 5 md. Both attenuation peaks (Figure 4a) and velocity transition zones (Figure 4b) shift towards larger R as permeability increases. This result is clear if we consider the fact that the fluid in its squirting motion can relax more easily if R is shorter and the permeability is higher.

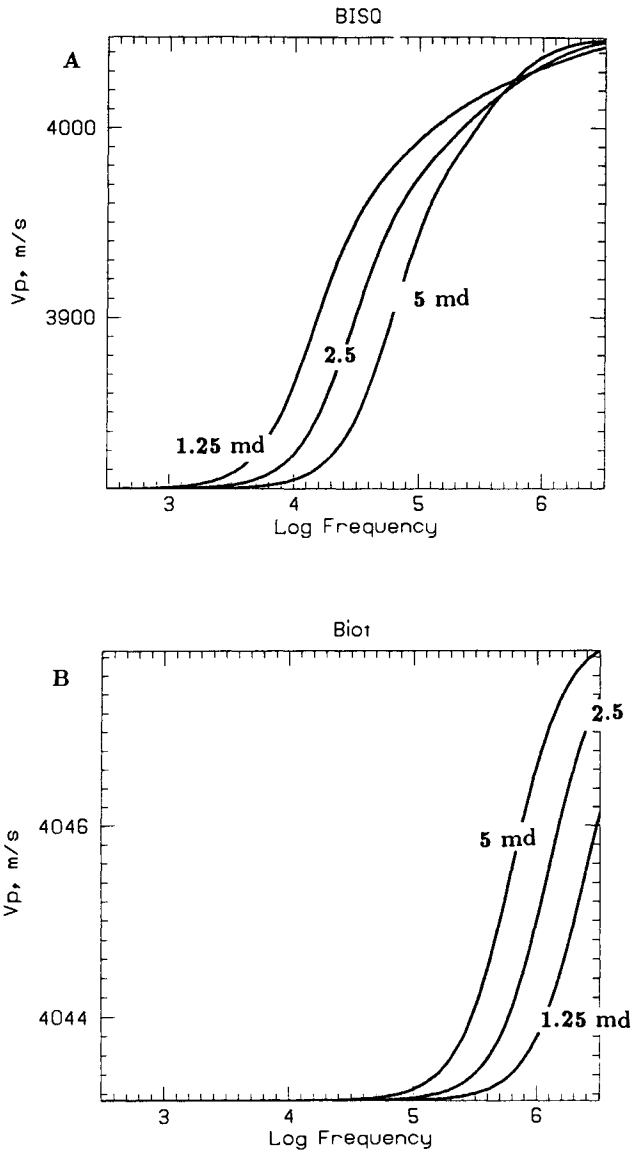

FIG. 2. The effect of frequency. (a) Compressional velocity versus frequency for permeability 1.25, 1.5, and 5 md, as predicted by the BISQ theory. (b) Compressional velocity versus frequency for permeability 1.25, 2.5, and 5 md from the original Biot theory.

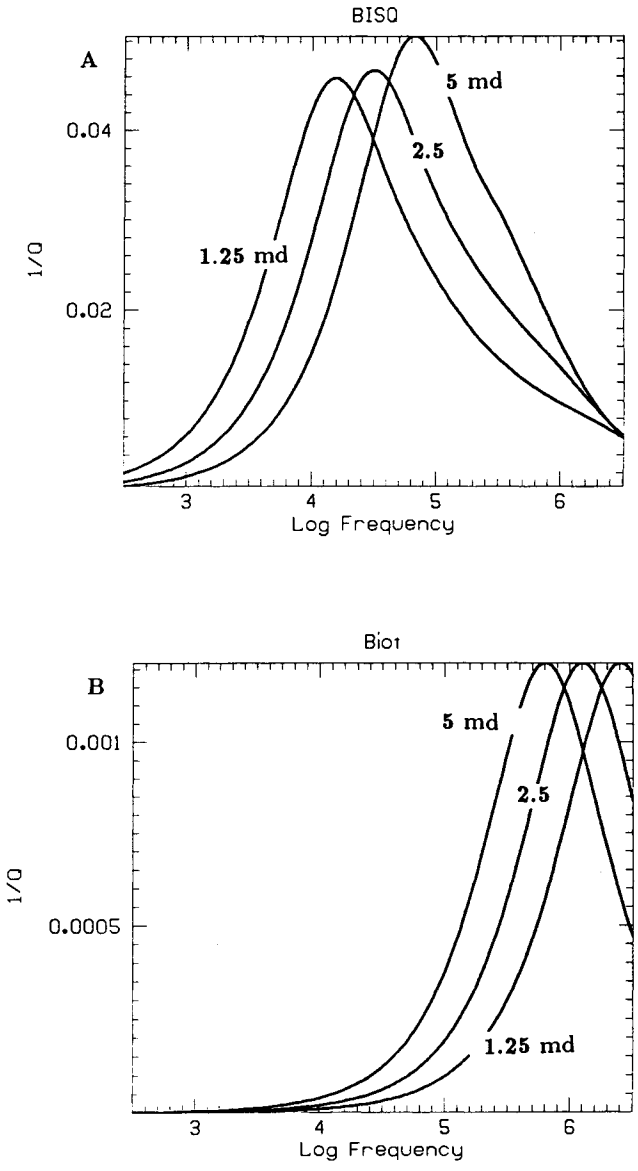

FIG. 3. The effect of frequency. (a) Inverse attenuation quality factor Q^{-1} versus frequency for permeability 1.25, 1.5, and 5 md, as predicted by the BISQ theory. (b) Q^{-1} versus frequency for permeability 1.5, 2.5, and 5 md from the original Biot theory.

APPLICATIONS OF THE BISQ THEORY

The BISQ theory allows us to realistically calculate attenuation and velocity dispersion in saturated rocks as functions of such important parameters as frequency, fluid viscosity, fluid compressibility, porosity, and permeability. An immediate application of this theory is in monitoring EOR processes where both the compressibility and the viscosity of pore fluids may change over time (Ito et al., 1979; Wang and Nur, 1990).

Consider for example a heavy oil reservoir subject to thermal EOR treatment. The viscosity of heavy oil may drop significantly with increasing temperature. We choose the parameters of the reservoir identical to those used in the above numerical examples. Its permeability is 10 md, the density of the heavy oil is 900 kg/m^3. We calculate compressional velocity V_P versus frequency for viscosities 10^4, 10^2, and 1 cps (Figure 5). At frequency 1 kHz (appropriate for cross-well tomography), V_P is 4014, 3938, and 3854 m/s for viscosities 10^4, 10^2, and 1 cps, respectively. Therefore, this velocity decrease can be directly interpreted in terms of changing temperature that provides a direct lead to EOR monitoring.

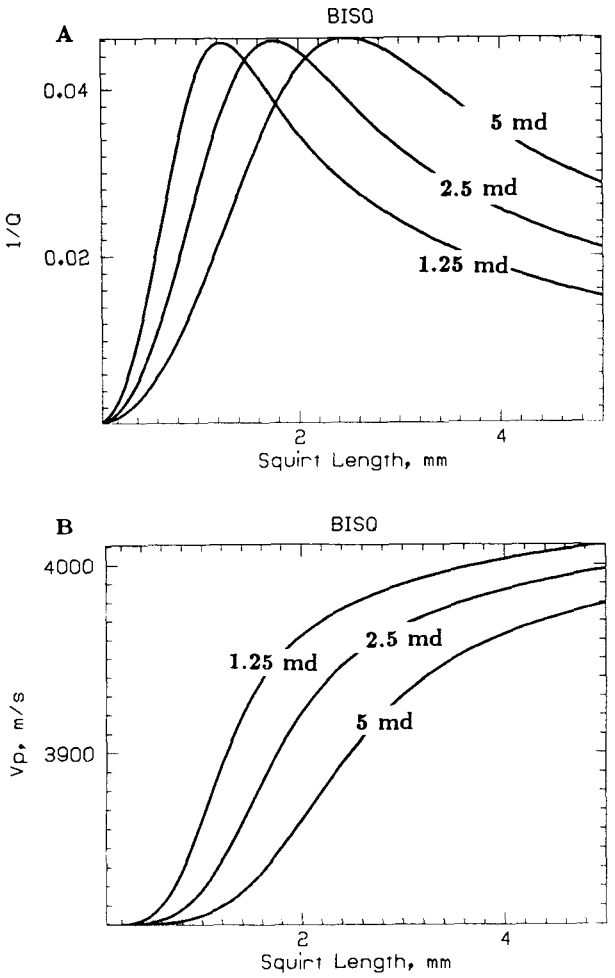

FIG. 4. The effect of characteristic squirt flow length at frequency 10 kHz. (a) Inverse attenuation quality factor Q^{-1} versus R for permeability 1.25, 2.5, and 5 md. (b) Compressional velocity versus R for permeability 1.25, 2.5, and 5 md.

To show that the BISQ model provides a means of estimating permeability based on seismic data, we attempted to simulate the experimental results of Klimentos and McCann (1990) where attenuation was recorded as a function of permeability for water-saturated sandstone samples of constant porosity 15 percent at frequency 1 MHz (17 samples). The properties of the dry skeletons vary significantly among these samples which is clear from the varying V_P (from 3933 to 5078 m/s), average grain size (from 72 to 377 μm), and clay content (from 0.002 to 0.15).

The goal of this example is to show principal qualitative correlation between the BISQ-predicted and measured results. Therefore, we choose fixed skeleton parameters for all samples by matching calculated V_P to the average measured value. These parameters are: K = 20 GPa, ν = 0.15, ρ_s = 2650 kg/m^3. We choose R = 0.17 mm by matching theoretical to observed attenuation values for one sample (permeability 2.21 md in this example). The theoretical results are in good qualitative correlation with the experimental data (Figure 6). Some mismatch at higher permeabilities can be explained by using average values for the skeleton's properties and R. As permeability increases, the attenuation rises to its intermediate permeability maximum and sharply drops afterwards to low values. This result explains the observed scatter of attenuation values at small permeability. The Biot theory fails to adequately model the experimental data as it yields unrealistically small attenuation values (Figure 6, lower curve).

The above example shows that attenuation appears to be a seismic property of sandstones that is the most sensitive to their permeability. This conclusion is consistent with the results of Akbar et al. (1993).

CONCLUSIONS

We presented a unified dynamic poroelasticity model for the propagation of P-waves in a porous elastic solid contain-

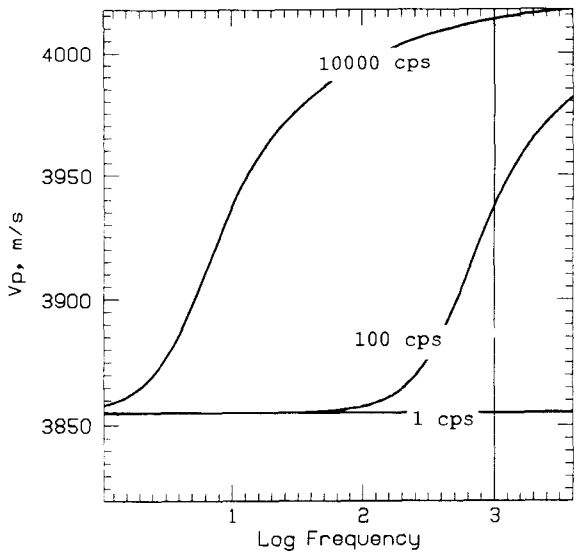

FIG. 5. The effect of viscosity. Compressional velocity V_P (m/s) versus frequency (Hz) for viscosities 10 000, 100, and 1 cps.

ing a compressible viscous fluid. The model takes into account two of the most important mechanisms of fluid/solid interaction: (1) the Biot mechanism where the fluid is forced to participate in the solid's motion by viscous friction and inertial coupling; and (2) the squirt mechanism where the fluid is being squeezed out of thin pores due to the solid's compression. The viscoelastic behavior of a saturated rock depends on two nondimensional groups. One is

$$\frac{\omega_c}{\omega} = \frac{\mu\phi}{k\rho_f\omega},$$

as in the original Biot theory. The second group is

$$\lambda R = \sqrt{R^2 \frac{\rho_f\omega^2}{F}\left(\frac{\phi + \rho_a/\rho_f}{\phi} + i\frac{\omega_c}{\omega}\right)},$$

which includes the characteristic squirt flow length R. For seismic frequencies, only one nondimensional group

$$\frac{R^2\omega\mu\phi}{kF}$$

determines the viscoelastic response of a rock. Both attenuation and velocity dispersion are strongly affected by the squirt flow. The BISQ model allows us to realistically calculate attenuation and velocity dispersion in saturated rocks as functions of frequency, fluid viscosity, fluid compressibility, porosity, and permeability. Therefore, this theory can be directly applied in monitoring EOR processes where both the compressibility and the viscosity of pore fluids change over time.

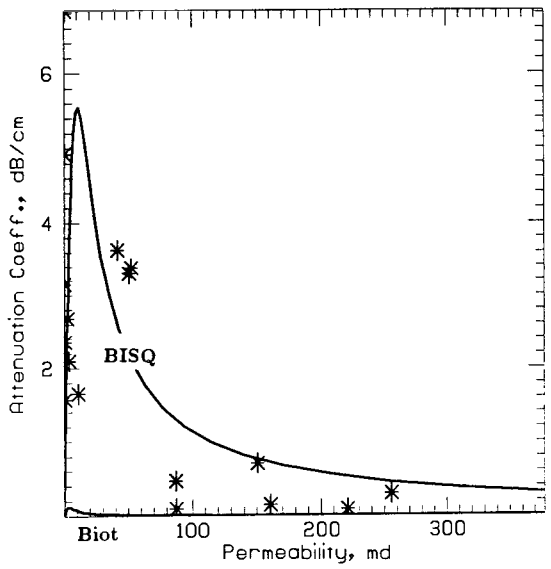

FIG. 6. The effect of permeability. Attenuation coefficient in dB/cm versus permeability from the BISQ theory (upper curve) and from the original Biot theory (lower curve); asterisks—experimental data from Klimentos and McCann (1990).

ACKNOWLEDGMENTS

The idea of merging the Biot and the squirt-flow mechanisms into a unified theory was suggested by Nabil Akbar. We thank Gary Mavko and J.-P. Blangy for helpful discussions. This work was sponsored by the Gas Research Institute Research Contract No. 5087-260-1635.

REFERENCES

Akbar, N., Dvorkin, J., and Nur, A., 1993, Relating P-wave attenuation to permeability: Geophysics, **58**, 20–29.
Berryman, J. G., 1980, Confirmation of Biot's theory: Appl. Phys. Lett., *37*, 382–384.
Biot, M. A., 1941, General theory of three-dimensional consolidation: J. Appl. Phys., **12**, 155–164.
——— 1942, Bending settlement of a slab resting on a consolidating foundation: J. Appl. Phys., **13**, 35–40.
——— 1956, Theory of propagation of elastic waves in a fluid-saturated porous solid. I. Low-frequency range, II. Higher frequency range: J. Acoust. Soc. Amer., **28**, no. 2, 168–191.
Burridge, R., and Keller, J., 1981, Poroelasticity equations derived from microstructure: J. Acoust. Soc. Am., **70**, no. 4, 1140–1146.
Gardner, G. H. F., 1962, Extensional waves in fluid-saturated porous cylinders: J. Acoust. Soc. Am., **34**, no. 1, 36–40.
Ito, H., DeVilbiss, J., and Nur, A., 1979, Compressional and shear waves in saturated rocks during water-steam transition: J. Geophys. Res., **84**(B9), 4731–4735.
Johnston, D. H., Toksöz, M. N., and Timur, A., 1979, Attenuation of seismic waves in dry and saturated rocks: II. Mechanisms: Geophysics, **44**, 691–711.
Klimentos, T., and McCann, C., 1990, Relationships among compressional wave attenuation, clay content, and permeability in sandstones: Geophysics, **55**, 998–1014.
Mavko, G., and Nur, A., 1975, Melt squirt in asthenosphere, J. Geophys. Res., **80**(11), 1444–1448.
——— 1979, Wave attenuation in partially saturated rocks: Geophysics, **44**, 161–178.
Miksis, M. J., 1988, Effect of contact line movement on the dissipation of waves in partially saturated rocks: J. Geophys. Res., **93**(B6), 6624–6634.
Murphy, W. F., Winkler, K. W., and Kleinberg, R. L., 1986, Acoustic relaxation in sedimentary rocks: Dependence on grain contacts and fluid saturation: Geophysics, **51**, 757–766.
Palmer, I. D., and Traviolia, M. L., 1980, Attenuation by squirt flow in undersaturated gas sands: Geophysics, **45**, 1780–1792.
Rice, J. R., and Cleary, M. P., 1976, Some basic stress diffusion solutions for fluid-saturated elastic porous media with compressible constituents: Rev. Geophys. and Space Phys., **14**, no. 2, 227–241.
Stoll, R. D., 1974, Acoustic waves in saturated sediments: *in* Hampton, L., Ed., Physics of sound in marine sediments: Plenum Press.
Toksöz, M. N., and Johnston, D. H., (Eds.), 1981, Seismic wave attenuation, Geophysics reprint series, 2: Soc. Expl. Geophys.
Wang, Z., and Nur, A., 1990, Dispersion analysis of acoustic velocities in rocks: J. Acoust. Soc. Am., **87**, no. 6, 2384–2395.
Wepfer, W. W., and Cristensen, N. I., 1990, Compressional wave attenuation in oceanic basalts: J. Geophys. Res., **95**(B11), 17 431–17 439.
White, J. E., 1983, Underground sound, Elsevier Science Publ.

APPENDIX

DYNAMIC POROELASTICITY (BIOT'S THEORY)

Relations among stresses and pressure

For uniaxial deformation in the x-direction (Figure 1b), total stresses in the solid-fluid system σ_x^t are related to a skeleton's deformation $e = du/dx$ as (Biot, 1941; Rice and Cleary, 1976):

$$\sigma_x^t = Me - \alpha P.$$

The total stresses σ_x^t are separated into two parts: stresses σ_x acting on the solid part of the rock and stresses $-\phi P$ acting on the fluid part (Biot, 1956):

$$\sigma_x^t = \sigma_x - \phi P.$$

By combining the above two equations, we obtain (1):

$$\sigma_x = M\frac{du}{dx} - \gamma P,\ \gamma = \alpha - \phi.$$

Dynamic equations

In the case under consideration, dynamic equations for a two-component solid-fluid continuum derived from Lagrange's equations with a dissipation function (Biot, 1956) are:

$$\rho_{11}u_{tt} + \rho_{12}w_{tt} + b(u_t - w_t) = \frac{\partial \sigma_x}{\partial x},$$

$$\rho_{22}w_{tt} + \rho_{12}u_{tt} - b(u_t - w_t) = -\phi P_x,$$

where $\rho_{11} = (1 - \phi)\rho_s + \rho_a$, $\rho_{12} = -\rho_a$, $\rho_{22} = \phi\rho_f + \rho_a$, and $b = \mu\phi^2/k$.

Substituting equation (1) into these dynamic equations we find:

$$(1 - \phi)\rho_s u_{tt} + \rho_a(u_{tt} - w_{tt}) + \frac{\mu\phi^2}{k}(u_t - w_t) = Mu_{xx} - \gamma P_x,$$

$$\phi\rho_f w_{tt} - \rho_a(u_{tt} - w_{tt}) - \frac{\mu\phi^2}{k}(u_t - w_t) = -\phi P_x.$$

This system can be linearly transformed into the equations (2):

$$(1 - \phi)\rho_s u_{tt} + \phi\rho_f w_{tt} = Mu_{xx} - \alpha P_x,$$

$$\phi\rho_f w_{tt} - \rho_a(u_{tt} - w_{tt}) - \frac{\mu\phi^2}{k}(u_t - w_t) = -\phi P_x.$$

Velocity and attenuation

For plane waves propagating in a homogeneous medium, the amplitude is given by $A(x, t) = A_0 e^{i(\ell x - \omega t)}$, where ω is the angular frequency and ℓ is the wavenumber. Attenuation may be introduced by allowing the wavenumber to be complex (Toksöz and Johnston, 1981): $\ell = \mathrm{Re}\,(\ell) + i\,\mathrm{Im}\,(\ell)$. Attenuation coefficient a and the phase velocity V_P are:

$$a = \mathrm{Im}\,(\ell),\ V_P = \omega/\mathrm{Re}\,(\ell).$$

The inverse quality factor Q^{-1} is related to a and V_P as:

$$Q^{-1} = 2aV_P/\omega.$$

To find attenuation and phase velocity, we look for the solution of system (2) and (6) in the following form:

$$u(x, t) = C_1 e^{i(\ell x - \omega t)},$$

$$w(x, t) = C_2 e^{i(\ell x - \omega t)},$$

$$P(x, t) = P_0 e^{i(\ell x - \omega t)}.$$

After substituting these equations into (2) and (6), and solving for constants C_1 and C_2, we arrive at the following linear system:

$$C_1\left[Y\frac{1}{\rho_2}\left(M + \frac{\alpha\gamma F}{\phi}\right) - \frac{\rho_1}{\rho_2}\right] + C_2\left(Y\frac{\alpha F}{\rho_2} - 1\right) = 0,$$

$$C_1\left(Y\frac{\gamma F}{\rho_2} + \frac{\rho_a}{\rho_2} + i\frac{\omega_c}{\omega}\right) + C_2\left(Y\frac{\phi F}{\rho_2} - 1 - \frac{\rho_a}{\rho_2} - i\frac{\omega_c}{\omega}\right) = 0,$$

where $Y = (\ell/\omega)^2$, $\rho_1 = (1 - \phi)\rho_s$, $\rho_2 = \phi\rho_f$.

The above system will have nonzero solutions for constants C_1 and C_2 only if its determinant is zero. This condition leads to the following equation for Y:

$$AY^2 + BY + C = 0,$$

which gives two solutions:

$$Y_{1,2} = -\frac{B}{2A} \pm \sqrt{\left(\frac{B}{2A}\right)^2 - \frac{C}{A}}.$$

Therefore, we arrive at two values for the ratio ℓ/ω:

$$X_{1,2} = \left(\frac{\ell}{\omega}\right)_{1,2} = \sqrt{Y_{1,2}},$$

as well as for wavenumber ℓ:

$$\ell_{1,2} = \omega X_{1,2}.$$

Thus we have two values for P-velocity (the fast wave and the slow wave) and two corresponding values for attenuation:

$$V_{p1,2} = \frac{1}{\mathrm{Re}\,(X_{1,2})},\ a_{1,2} = \omega\,\mathrm{Im}\,(X_{1,2}).$$